



This is a repository copy of *Avalanche Noise in AlO.52In0.48P Diodes*.

White Rose Research Online URL for this paper:  
<http://eprints.whiterose.ac.uk/99292/>

Version: Accepted Version

---

**Article:**

Qiao, L., Cheong, J.S., Ong, J.S.L. et al. (4 more authors) (2015) Avalanche Noise in AlO.52In0.48P Diodes. IEEE Photonics Technology Letters, 28 (4). pp. 481-484. ISSN 1041-1135

<https://doi.org/10.1109/LPT.2015.2499545>

---

© 2015 IEE. Personal use of this material is permitted. Permission from IEEE must be obtained for all other users, including reprinting/ republishing this material for advertising or promotional purposes, creating new collective works for resale or redistribution to servers or lists, or reuse of any copyrighted components of this work in other works.

**Reuse**

Unless indicated otherwise, fulltext items are protected by copyright with all rights reserved. The copyright exception in section 29 of the Copyright, Designs and Patents Act 1988 allows the making of a single copy solely for the purpose of non-commercial research or private study within the limits of fair dealing. The publisher or other rights-holder may allow further reproduction and re-use of this version - refer to the White Rose Research Online record for this item. Where records identify the publisher as the copyright holder, users can verify any specific terms of use on the publisher's website.

**Takedown**

If you consider content in White Rose Research Online to be in breach of UK law, please notify us by emailing [eprints@whiterose.ac.uk](mailto:eprints@whiterose.ac.uk) including the URL of the record and the reason for the withdrawal request.



[eprints@whiterose.ac.uk](mailto:eprints@whiterose.ac.uk)  
<https://eprints.whiterose.ac.uk/>

# Avalanche Noise in $\text{Al}_{0.52}\text{In}_{0.48}\text{P}$ Diodes

L. Qiao, J. S. Cheong, J. S. L. Ong, J. S. Ng Member, IEEE, A. B. Krysa, J. E. Green and J. P. R. David, Fellow, IEEE

**Abstract**— Multiplication and avalanche excess noise measurements have been undertaken on a series of AllnP homo-junction PIN and NIP diodes with *i* region widths ranging from 0.04  $\mu\text{m}$  to 0.89  $\mu\text{m}$ , using 442 and 460 nm wavelength light. Low dark currents of  $< 170 \text{ nA cm}^{-2}$  at 95% of breakdown voltage were obtained in all the devices because of its wide bandgap and there was no tunneling dark current present even at high-fields  $> 1000 \text{ kV/cm}$ . For a given multiplication factor, the excess noise decreased as the avalanche width decreased due to the ‘dead-space’ effect. Using 460 nm wavelength light, measurements showed that a separate absorption multiplication avalanche photodiode (SAM-APD) with a nominal multiplication region width of 0.2  $\mu\text{m}$  had an effective *k* (hole to electron ionization coefficient ratio) of  $\sim 0.3$ .

**Index Terms**—Avalanche photodiodes, avalanche multiplication, excess noise, impact ionization, AllnP, narrow band detector

## I. INTRODUCTION

Optical underwater communication systems require a high-sensitivity detector with a peak responsivity at approximately 480 nm, as this corresponds to the maximum transmittance in seawater [1]. There are several semiconductor materials which can detect light at 480 nm, such as Si and GaP [2, 3], however these also have a broad spectral response and so will be sensitive to the presence of extraneous light sources at other wavelengths. Using these broadband detectors will require optical band-pass filters with a high rejection ratio and center wavelength of  $\sim 480 \text{ nm}$ , which add cost and complexity to the system. Consequently an inherently narrow spectral response photodetector is preferred. Zhang et al. [4] demonstrated that an  $\text{Al}_{0.52}\text{In}_{0.48}\text{P}$  (hereafter AllnP) PIN photovoltaic detector with a  $\text{Ga}_{0.52}\text{In}_{0.48}\text{P}$   $\text{p}^+$  cladding has a peak spectral response at 480 nm and a full-width-half-maximum (FWHM) of 45 nm. Later, Cheong et al. reported on the photo-response of an AllnP homo-junction PIN diode with a narrower FWHM of 22 nm and an effective responsivity of 18 A/W, with a multiplication factor of 167 at  $\sim 480 \text{ nm}$  [5]. This was achieved by employing thick  $\text{p}^+$  AllnP cladding, which yields small FWHM but has the undesirable

effect of the peak responsivity. Exploiting multiplication factor from the diode however allow them to eventually achieve excellent responsivity value in [5].

Although avalanche multiplication can increase the sensitivity of an optical receiver, the maximum useful gain is ultimately limited by the associated excess noise that originates from the stochastic nature of the impact ionization process. For thick avalanching structures, where the carriers can be assumed to be in equilibrium with the electric field, the excess noise factor (F) was described by McIntyre [6] as

$$F = kM + (1-k)\left(2 - \frac{1}{M}\right) \quad (1)$$

where  $k = \beta/\alpha$  for the case of pure electron initiated multiplication.  $\alpha$  and  $\beta$  are ionization coefficients for electrons and holes respectively and they are the reciprocal of the average distance that a carrier travels before initiating an impact ionization event.

The ionization coefficients measured by Ong et al. [7] showed that  $\beta/\alpha$  is 0.4 - 1.0 over the electric-field range of 400-1300 kV/cm consequently equation (1) would suggest that AllnP should exhibit high excess noise and that any amplification of the photocurrent due to impact ionization would be matched by an almost similar increase in the excess noise, thereby not improving the overall sensitivity of the system.

However, it is now well known, both experimentally and theoretically [8-10] that, for a given *M*, the excess noise reduces with decreasing avalanche layer thickness due to the increasing significance of the carrier ‘dead space’, defined as the minimum distance a carrier has to travel in the direction of the electric-field to gain the ionization threshold energy. This dead space has the effect of reducing the randomness in where carriers ionize and hence reduces the excess noise. The beneficial effects of the dead-space increases as the avalanching width reduces and the lower limit that can be practically utilized is determined by dark currents due to quantum mechanical tunneling across the band gap at high electric fields, i.e. the tunneling current. Being the widest bandgap material which can be grown lattice matched to GaAs, and having an indirect band gap, AllnP is expected to have negligible tunneling effect even at high-fields  $> 1 \text{ MV/cm}$  and therefore it should be possible to utilize a thin avalanche layer to give low dark currents and low excess noise simultaneously.

L. Qiao, J. S. Cheong, J. S. Ng, A. B. Krysa, J. E. Green and J. P. R. David are with the Department of electronic and electrical engineering, University of Sheffield, Mappin Street, Sheffield, S1, 3JD, UK. (e-mail: [lqiao1@sheffield.ac.uk](mailto:lqiao1@sheffield.ac.uk), [j.s.cheong@shef.ac.uk](mailto:j.s.cheong@shef.ac.uk), [j.s.ng@sheffield.ac.uk](mailto:j.s.ng@sheffield.ac.uk), [a.krysa@sheffield.ac.uk](mailto:a.krysa@sheffield.ac.uk), [j.e.green@sheffield.ac.uk](mailto:j.e.green@sheffield.ac.uk), [j.p.david@shffield.ac.uk](mailto:j.p.david@shffield.ac.uk)).

J. S. L. Ong is now with the Microelectronic Engineering Department, University of Malaya Perlis, Pauh Putra Campus, 02600 Arau, Perlis, Malaysia (e-mail: [slong@unimap.edu.my](mailto:slong@unimap.edu.my)).

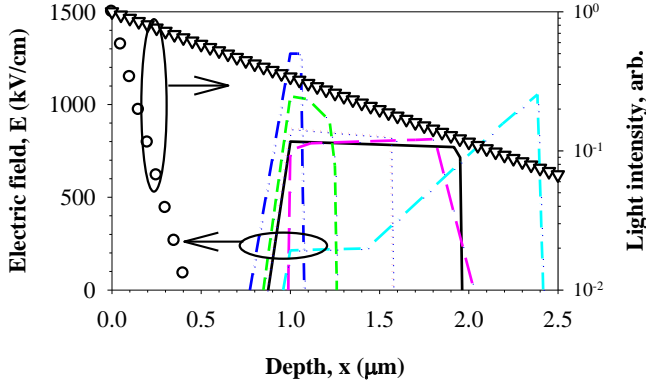


Fig. 1 Simulated electric field profiles in PINs ( $w = 1.0, 0.5, 0.2, 0.04 \mu\text{m}$ ), a NIP ( $w = 0.8 \mu\text{m}$ ) and the SAM-APD using the results obtained from capacitive-voltage measurement shown as solid, dotted, short-dashed, dashed-dot-dot, long-dashed and dashed-dot lines. Also illustrate the absorption profiles of 442 and 480 nm, ie. the light attenuation vs distance, as circles and triangles.

There are however no experimental reports of excess noise for AlInP. In this paper, we present excess noise data obtained from a series of AlInP PIN and NIP diodes with nominal avalanche layer thickness ranging from 0.04 to 1.0  $\mu\text{m}$ . Excess noise measurements of a Separate-Absorption and Multiplication APD (SAM-APD) with a nominal 0.2  $\mu\text{m}$  avalanche layer are also reported.

## II. SAMPLE DETAILS AND CHARACTERIZATION

The series of diodes used in this work include the three homo-junction PINs and a NIP structure with nominal  $i$  region widths,  $w$  of 0.2, 0.5, 1.0, and 0.8  $\mu\text{m}$ , respectively, previously reported in the work of [7]. This work also includes a PIN which has a nominal  $i$  region thickness of 0.04  $\mu\text{m}$  and the SAM-APD reported in [5]. To ensure that the incident light is not attenuated by the 50 nm heavily doped GaAs contacting layer, it was selectively etched from the central window region of the circular mesa devices. As excess noise measurements can be sensitive to any ‘mixed’ carrier injection into the high

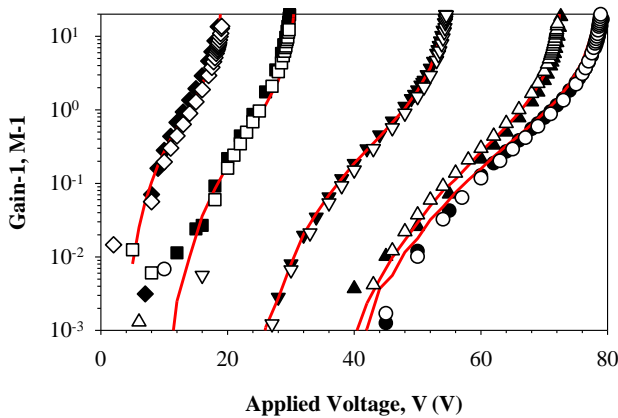


Fig. 2. Experimental  $M-1$  versus reverse Bias for AlInP PIN diodes using 442 nm laser (close symbol) and 460 nm LED (open symbol) with  $w = 0.04 \mu\text{m}$  ( $\blacklozenge, \blacklozenge$ ), 0.2  $\mu\text{m}$  ( $\blacksquare, \square$ ), 0.5  $\mu\text{m}$  ( $\blacktriangledown, \blacktriangledown$ ) and 1.0  $\mu\text{m}$  ( $\bullet, \circ$ ) and NIP diodes with  $w = 0.8 \mu\text{m}$  ( $\blacktriangle, \triangle$ ). Solid lines are modelled results assuming 442 nm illumination.

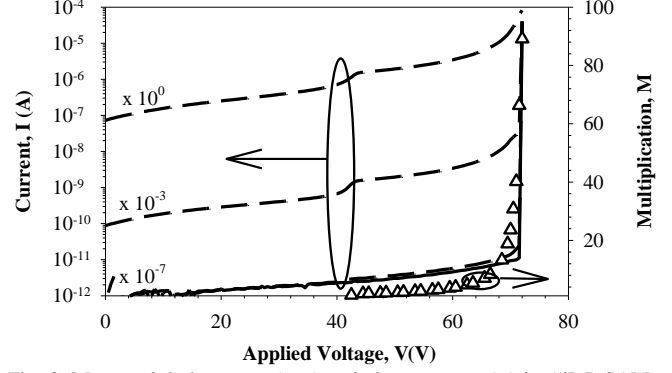


Fig. 3. Measured dark current (—) and photocurrents (--) in AlInP SAM-APD under 460 nm LED illumination with the optical power attenuated by  $10^0, 10^3$  and  $10^7$ . Also shown is the corresponding gain as a function of bias voltage.

field region, the mesa sidewalls were passivated and covered by metal to prevent any edge illumination during the measurement.

From the dark current-voltage measurements, no tunneling current was observed even in the thinnest ( $w = 0.04 \mu\text{m}$ ) diode structure. Capacitance-voltage (C-V) measurements revealed that the doping densities in  $p^+$  and  $n^+$  claddings in all structures are  $\sim 3 \times 10^{17} \text{cm}^{-3}$  and  $\sim 4 \times 10^{18} \text{cm}^{-3}$ , similar to those reported in [7]. Using the C-V data and solving Poisson’s equation, electric field profiles in these structures were simulated at their corresponding breakdown voltages, as shown in Fig. 1. The total depletion widths are thicker than the nominal  $i$  thicknesses due to the relatively low doping densities in the  $p^+$  claddings which results in a significant depletion into the  $p^+$  cladding layers, especially in the thinnest PIN. For simplicity, we will refer to just their nominal thicknesses in the subsequent text. Using a white light source and a monochromator, the peak of the spectral response in all the devices was found to be  $\sim 480 \text{nm}$  with a FWHM of  $\sim 22 \text{nm}$ .

## III. RESULTS

Multiplication and excess noise measurements were undertaken using a 442 nm He-Cd laser and a Thorlab LED470L LED with a 460 nm peak emission [11]. The latter offers the closest emission wavelength available in commercial LEDs with a reasonable output power to 480 nm. The measurements were performed using the setup described in Lau et al. [12]. The transimpedance amplifier (TIA), based on the Analogue Devices AD9631 with a gain of 2200 V/A (unterminated) was used to convert current into a voltage. The output of the TIA was then amplified by the Minicircuits ZFL-500LN+ and fed into a bandpass filter SBP-10.7+, which had a pass band centred around 10 MHz and a bandwidth of 4.2 MHz.

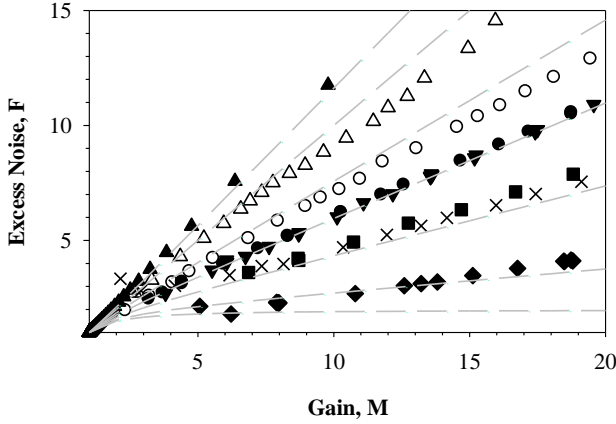


Fig. 4. Experimental  $F$  versus  $M$  using 442 nm laser (closed symbol) and 460 nm LED (open symbol) for AllInP PIN diodes with  $w = 0.04 \mu\text{m}$  ( $\square$ ),  $0.2 \mu\text{m}$  ( $\blacksquare$ ) and  $1.0 \mu\text{m}$  ( $\bullet$ ,  $\circ$ ), NIP diodes with  $w = 0.8 \mu\text{m}$  ( $\blacktriangle$ ,  $\triangle$ ) and SAM-APD ( $\times$ ). Grey lines are McIntyre's curves with  $k = 0, 0.1, 0.3, 0.5, 0.7, 1$  and  $1.2$ .

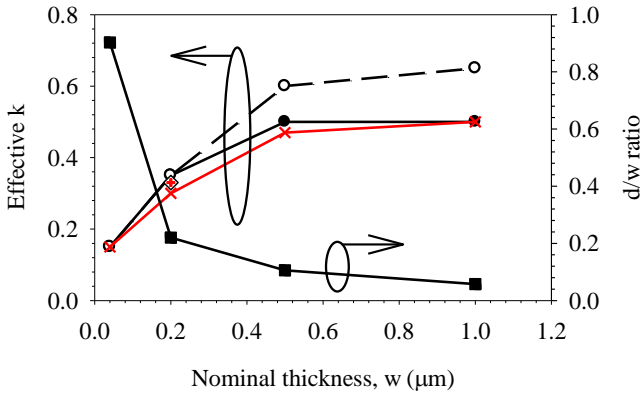


Fig. 5.  $k_{\text{eff}}$  versus nominal width using 442 nm laser ( $\bullet$ ) and 460 nm LED ( $\circ$ ) for AllInP PIN diodes. The symbol ( $\diamond$ ) represents  $k_{\text{eff}}$  of the SAM-APD by using 460 nm LED. The symbols ( $\times$  and  $+$ ) show PIN modelling results by using pure injection and SAM-APD modelling results by using mixed injection respectively. Also shown the calculated  $d/w$  ratio, by taking the highest electric fields attainable in these devices shown in Fig. 1. Lines are the guide to the eyes.

The excess noise factor,  $F$ , obtained using the expression:

$$F(M) = \frac{N_{\text{DUT}}}{aMI} \times \frac{B_{\text{eff}}(C_{\text{si}})}{B_{\text{eff}}(C_{\text{DUT}})} \quad (2)$$

where  $a$  is a correction factor,  $I$  is the multiplied photocurrent,  $B_{\text{eff}}(C_{\text{si}})$  is the effective noise bandwidth of calibrating Si photodiode and  $B_{\text{eff}}(C_{\text{DUT}})$  is the effective noise bandwidth at the device under test's capacitance. To ensure the dark current does not affect the measurements especially at high gains, optical sources were modulated and the resulting photocurrents and noise power were measured using lock in amplifiers.

To determine if the multiplication characteristics obtained from these light sources are initiated by a single carrier type or otherwise, the absorption profiles for 442 and 480 nm wavelength photons in AllInP were calculated using the absorption coefficients from [13] as illustrated in Fig. 1. For

442 nm wavelength, > 99.9% of photons are absorbed in the  $1.0 \mu\text{m}$  top doped cladding layer, giving virtually pure electron (or hole) initiated multiplication. For the 460 nm emission from the LED, due to the relatively short diffusion lengths in the doped AllInP, most of the photocurrent is contributed by the longer wavelength components of the LED spectrum absorbed within the depletion region. This results in a significant mixed carrier multiplication characteristic. Fig. 2 shows the multiplication characteristics obtained in the PINs (NIP) plotted as  $\log(M-1)$ , to emphasize the low field multiplication characteristics. As  $\beta/\alpha \sim 0.7$ , even at low fields, the difference between 442 nm and 460 nm appears almost indistinguishable, especially in the thinner avalanching structures. The maximum gain in these devices is  $\sim 20$  probably due to un-optimized etching process in these mesa devices, resulting in high electric field at the mesa edges [14].

Fig. 3 shows the dark current, photocurrent and multiplication for the AllInP SAM-APD using the 460 nm LED. The dark current is less than 10 pA at 99 % of the breakdown voltage for a 210  $\mu\text{m}$  radius device. Such a low dark current in the device allows the direct measurement of photocurrent even when the optical power was attenuated by  $10^7$  down to  $\sim 1$  pW. There is no tunneling current despite the peak electrical field exceeding 1 MV/cm and the multiplication – voltage ( $M$ - $V$ ) curve shows a gain of 90 can be obtained. The multiplication here however, was measured using only the 460 nm LED as due to the thick cladding and absorption regions, most of the photons were absorbed before entering the high-field region and therefore can be assumed to be initiated by electrons only.

Fig. 4 shows the excess noise-multiplication characteristics for the AllInP PIN and NIP structures using 442 nm laser illumination. Also shown are the excess noise characteristics for the thickest PIN and NIP, together with the results from the SAM-APD obtained using 460 nm illumination. The grey lines correspond to the McIntyre noise theory based on the  $\beta/\alpha$  ( $k$ ) ratio. The excess noise factors of the mixed injection (460 nm) are higher than the pure electron injection (442 nm) in the  $1.0 \mu\text{m}$  PIN structure as the contribution of holes to the multiplication process is detrimental. The opposite behavior is seen in the  $0.8 \mu\text{m}$  thick NIP structure where the highest noise is obtained with the use of 442 nm laser excitation with holes initiating multiplication, compared to when 460 nm was used. From the ionization coefficient ratio,  $k$  should vary from  $\sim 0.6$  for the thickest structure investigated here to  $\sim 1$  for the thinner structures, in contrast to the experimental results. Decreasing the  $w$  in the PIN structures, results in the excess noise decreasing to levels corresponding to  $k = 0.32$  and  $k = 0.11$ , in the  $0.2$  and  $0.04 \mu\text{m}$  structures respectively. The results of the pure injection and mixed injection (not shown) are quite similar in these thin structures, because the impact ionization coefficients  $\alpha$  and  $\beta$  are almost identical when the width is less than  $0.5 \mu\text{m}$  [7]. The excess noise of the SAM-APD are close to  $k = 0.3$  as seen in Fig. 4 and in agreement with the data from the PIN with the  $0.2 \mu\text{m}$  nominal i region width.

#### IV. MODELLING & DISCUSSION

Simulation of  $M(V)$  and  $F(M)$  in the presence of a dead-space can be implemented using a method initially proposed by Hayat et al. [15] or the random-path length (RPL) model [16]. The latter was used in this work. To account for the non-uniform electric field profile in these devices, the electron ionization probability density,  $h_e(x_0, x)$  which describes the ionizing probability of an electron at  $x_0$  after travelling a distance  $x$  can be expressed as [17]

$$h_e(x_0, x) = \begin{cases} 0 & , x \leq d_e(x_0) \\ \alpha^*(x + x_0) \exp\left[-\int_{d_e(x_0)}^x \alpha^*(z + x_0) dz\right] & , x > d_e(x_0) \end{cases} \quad (3)$$

In (3),  $d_e(x_0)$  is the distance of the dead-space, which is derived from the threshold energy,  $E_{\text{the}}$  and electric field,  $\xi$  given by

$$E_{\text{the}} = \int_{d_e(x_0)}^x \xi(x) dx \quad (4)$$

By integrating (3), the probability of an electron not ionizing after travelling a distance  $x$  from  $x_0$ ,  $r$  is expressed as

$$\ln(r) = - \int_{d_e(x_0)}^x \alpha^*(z + x_0) dz \quad (5)$$

where  $0 < r < 1$  determines the electron (hole) ionizing length. The multiplication can be easily computed after all the carriers exit the depletion width. The expressions for holes are easily obtained by replacing  $\alpha^*$ ,  $d_e$  and  $E_{\text{the}}$  with  $\beta^*$ ,  $d_h$  and  $E_{\text{thh}}$  respectively. The depletion width was discretized into a suitable mesh to calculate  $d_e$  ( $d_h$ ) and  $\alpha^*(\beta^*)$ . The simulation was repeated until the multiplication value converges. The excess noise factor,  $F$  is given by  $\langle M^2 \rangle / \langle M \rangle^2$ .

The enabled ionization coefficients  $\alpha^*(\beta^*)$ , were obtained from the local parameterized ionization coefficients,  $\alpha'(\beta')$  using a simple correction  $\frac{1}{\alpha^*} = \frac{1}{\alpha'} - 2d_e$  and  $\frac{1}{\beta^*} = \frac{1}{\beta'} - 2d_h$  [16], where both  $\alpha'(\beta')$  and  $d_e(d_h)$  can be found in [18]. The simulations were done assuming a pure single carrier initiated multiplication, ie. 442 nm illumination, using the electric field profile shown in Fig. 1. There appears to be good agreement between the simulated multiplication and experimentally determined values over a wide dynamic range, even in thinnest devices where the dead space effect is significant, as shown by the solid lines in Fig. 2. To show this more clearly,  $d/w$  in these devices is plotted in Fig. 5, where the dead-space occupies an increasing fraction of the device width in the thinner devices. Simulations of the excess noise also gave good agreement to the experimental results shown in Fig. 4 (not shown). To show this more clearly, effective  $k$  (as defined by the McIntyre model) is plotted against the nominal  $i$  region width, obtained from the experimental measurements and the simulations as illustrated in Fig. 5. From this figure we can

see that the excess noise of the SAM-APD is equivalent to that of a 0.2  $\mu\text{m}$  PIN, despite having a much wider triangular electric field profile as shown in Fig. 1.

The modelling also shows that in the thinnest PIN structure investigated, the effective  $k$  corresponds to 0.15, comparable to a good silicon based APD. A properly designed SAM-APD with a similarly thin avalanching region and a 2  $\mu\text{m}$  thick absorbing region should therefore ensure a device with a high responsivity, low noise and a relatively low operating voltage. Such a device with a 0.4 mm diameter (in order to achieve high responsivity) would have a capacitance of  $\sim 6.2$  pF when fully depleted, enabling a RC time limited bandwidth of  $\sim 513$  MHz at unity gain, making it suitable for underwater communication applications.

#### REFERENCES

- Giles, J.W. and I.N. Bankman. Underwater optical communications systems. Part 2: basic design considerations. in Military Communications Conference, 2005. MILCOM 2005. IEEE, 2005.
- McIntosh, D., et al., Flip-Chip Bonded GaP Photodiodes for Detection of 400- to 480-nm Fluorescence. *Photonics Technology Letters, IEEE*, 2011. **23**(13): p. 878-880.
- Melchior, H., et al., Atlanta fiber system experiment: Planar epitaxial silicon avalanche photodiode. *Bell System Technical Journal, The*, 1978. **57**(6): p. 1791-1807.
- Yonggang, Z., et al., GaInP-AlInP-GaAs Blue Photovoltaic Detectors With Narrow Response Wavelength Width. *Photonics Technology Letters, IEEE*, 2010. **22**(12): p. 944-946.
- Cheong, J.S., et al.,  $\text{Al}_{0.52}\text{In}_{0.48}\text{P}$  SAM-APD as a Blue-Green Detector. *Selected Topics in Quantum Electronics, IEEE Journal of*, 2014. **20**(6): p. 142-146.
- McIntyre, R.J., Multiplication noise in uniform avalanche diodes. *Electron Devices, IEEE Transactions on*, 1966. **ED-13**(1): p. 164-168.
- Ong, J.S.L., et al., Impact Ionization Coefficients in  $\text{Al}_{0.52}\text{In}_{0.48}\text{P}$ . *Electron Device Letters, IEEE*, 2011. **32**(11): p. 1528-1530.
- Hu, C., et al., Noise characteristics of thin multiplication region GaAs avalanche photodiodes. *Applied Physics Letters*, 1996. **69**(24): p. 3734-3736.
- Li, K.F., et al., Avalanche multiplication noise characteristics in thin GaAs  $p^+i-n^+$  diodes. *Electron Devices, IEEE Transactions on*, 1998. **45**(10): p. 2102-2107.
- Ong, D.S., et al., Full band Monte Carlo modeling of impact ionization, avalanche multiplication, and noise in submicron GaAs  $p^+i-n^+$  diodes. *Journal of Applied Physics*, 2000. **87**(11): p. 7885-7891.
- LED with Ball Lens LED470L. 2011; Available from: <http://www.thorlabs.de/thorcat/22300/LED470L-SpecSheet.pdf>.
- Lau, K.S., et al., Excess noise measurement in avalanche photodiodes using a transimpedance amplifier front-end. *Measurement Science and Technology*, 2006. **17**(7): p. 1941.
- Cheong, J.S., et al., Determination of absorption coefficients in AlInP lattice matched to GaAs. *Journal of Physics D: Applied Physics*, 2015. **48**(40): p. 405101.
- Beck, A.L., et al., Edge breakdown in 4H-SiC avalanche photodiodes. *Quantum Electronics, IEEE Journal of*, 2004. **40**(3): p. 321-324.
- Hayat, M.M., B.E.A. Saleh, and M.C. Teich, Effect of dead space on gain and noise of double-carrier-multiplication avalanche photodiodes. *Electron Devices, IEEE Transactions on*, 1992. **39**(3): p. 546-552.
- Ong, D.S., et al., A simple model to determine multiplication and noise in avalanche photodiodes. *Journal of Applied Physics*, 1998. **83**(6): p. 3426-3428.
- Ramirez, D.A., et al., Non-Local Model for the Spatial Distribution of Impact Ionization Events in Avalanche Photodiodes. *Photonics Technology Letters, IEEE*, 2014. **26**(1): p. 25-28.
- Cheong, J.S., et al., Relating the Experimental Ionization Coefficients in Semiconductors to the Nonlocal Ionization Coefficients. *Electron Devices, IEEE Transactions on*, 2015. **62**(6): p. 1946-1952.